Available online at www.sciencedirect.com
SCIENCE DIRECT®
Journal of Sound and Vibration 283 (2005) 645–663
JOURNAL OF SOUND AND VIBRATION
www.elsevier.com/locate/jsvi

Effect of sheared grazing mean flow on acoustic transmission in perforated pipe mufflers

E. Dokumaci*

Department of Mechanical Engineering, Dokuz Eylul University, Bornova, Izmir, Turkey

Received 7 November 2003; received in revised form 5 March 2004; accepted 5 May 2004
Available online 18 November 2004

Abstract

At present there are two competing numerical approaches for practical one-dimensional acoustical analyses of perforated pipe muffler components, namely, the discrete approach and the continuous approach. In a recent experiment (Journal of Sound and Vibration 265 (2003) 109) on the measurement of the elements of the transfer matrix across a perforate row with a subsonic low Mach number grazing mean flow, a discrepancy is observed between the experimental data and the prediction of a discrete approach. The present analysis shows that this discrepancy can be corrected by including an effect of the mean flow velocity profile, which is neglected in the current discrete methods as well as the distributed parameter method. Accordingly, the paper develops, for the first time, a quasi-one-dimensional theory of sound transmission in a perforated pipe carrying sheared grazing mean flow. The distinguishing features of this theory are the inclusion of the mean flow velocity in the sense of cross-sectional average and the introduction of slip flow velocity at the perforate wall. Two alternative formulations of the theory are presented. The proper formulation should necessarily be based on continuity, momentum and energy equations for one-dimensional acoustic perturbations. The simpler approximate formulation, which assumes isentropic wave propagation and neglects the energy equation, is shown to represent the proper formulation accurately for subsonic low Mach numbers. The current discrete and distributed parameter methods are reformulated on the basis of the proposed theory. Both the parallel and co-axial perforated multiple pipe elements are considered and the effect of mean flow velocity profile and slip velocity is shown by application to a straight-through resonator.

*Tel.: +90 232-388-7863; fax: +90 232-388-7864.
E-mail address: dokumaci@deu.edu.tr (E. Dokumaci).

0022-460X/$ - see front matter © 2004 Elsevier Ltd. All rights reserved.
doi:10.1016/j.jsv.2004.05.018

1. Introduction

Sound transmission in a perforated pipe, which is a common silencing element in automotive exhaust lines, have received the attention of a large number of authors. A considerable proportion of this work is devoted to the development of simplified mathematical models, as the practical usefulness of general numerical methods such as FEM or BEM is limited due to their computational overhead. Accordingly, the plane wave approximation is popular in analysis of mufflers with perforated pipes, as it can provide sufficiently accurate predictions for frequencies of interest in automotive applications. A further simplification is often provided in previous studies by assuming zero or uniform mean flow, although mean shear flow is always present in most applications to some degree. At present there are two competing numerical approaches for practical acoustical analyses of perforated pipe muffler components, namely, the discrete approach [1–3] and the continuous approach [4–8]. In the continuous approach, which is also known as the distributed parameter method, the perforations are modeled as distributed around the pipe wall continuously, whereas in the discrete approach they are modeled row by row.

In a recent paper, Aurégan and Leroux [9] presented a critical study of the existing discrete methods for perforated pipes carrying grazing mean flow. Having found that their measurements do not agree with the predictions of the discrete method of Sullivan [1], which is often referred to briefly as the segmentation method, they have proposed an empirical discrete model that fits the experimental data very closely and attributed the source of the discrepancy to the fluid viscosity causing some momentum transfer from the main flow to the tube wall, which is not taken into account in the segmentation method. Aurégan et al. [10] have studied this effect of the fluid viscosity on the wall boundary conditions in lined ducts carrying a parallel shear flow, however, it is not quite obvious how a similar analysis can be related to plane sound wave motion in a perforated pipe.

The predictions of the discrete method, and the continuous method for that matter, are dependent on the perforate impedance model used in calculations. Usually, suitable empirical or semi-empirical perforate impedance models have to be adopted for satisfactory predictions. But, in Ref. [9], by employing an ingenious device, the authors have eliminated the need for such impedance tuning. Therefore, the observed discrepancy should be related to a flaw in the basic formulation, and the present paper aims to propose that this flaw pertains to the assumption of the existing theory that the mean flow carried by a perforated pipe has a uniform velocity profile over the tube cross-sectional area.

In a hard-walled uniform pipe, the actual mean flow velocity profile may vary from a parabolic shape, characterizing a laminar flow, to a flatter shape characterizing a fully developed turbulent flow, with the no-slip condition satisfied at the pipe wall. Nevertheless, insofar as plane isentropic sound wave propagation is concerned, it is usually satisfactory to assume that the mean flow has a uniform velocity profile over the duct cross-section [11].

In a uniform perforated pipe, on the other hand, the form of the actual mean flow velocity profile is more difficult to characterize, as the pipe wall consists of rows of perforate holes separated by solid pipe sections. In the regions of perforate rows, it is plausible to presume some slip flow at the pipe wall due to the presence of open space and the walls of the solid pipe sections cannot be specified as exact no-slip regions due to transitional effects from the adjacent perforate rows. This is a complex enough picture to defy any first attempt to characterize the actual shape of

the mean flow velocity profile, however, it is clear that, the presence of some slip flow has to be allowed for in the analyses and, consequently, the commonly made assumption of uniform mean flow velocity profile requires further investigation. Accordingly, the present paper proposes a quasi-one-dimensional theory for sound transmission in a perforated pipe carrying a grazing parallel shear flow.

The distinguishing features of the new theory are the inclusion of the mean flow velocity profile in the sense of cross-sectional average and the introduction of slip flow at the perforate wall. Two alternative formulations are presented. The proper formulation should necessarily be based on continuity, momentum and energy equations for one-dimensional acoustic perturbations. The simpler approximate formulation, which assumes isentropic wave propagation and neglects the energy equation, is shown to represent the proper formulation accurately for subsonic low Mach numbers.

The present paper also presents reformulation of the existing discrete and continuous methods on the basis of the proposed theory. The discrete implementation of the proposed theory adopts the approach of Ref. [3] and is shown to predict the empirical model disclosed by Aurégan and Leroux [9]. The distributed parameter implementation, on the other hand, adopts the matrizant approach of Ref. [7]. Both the parallel and co-axial perforated multiple pipe elements are considered and the effect of mean flow velocity profile and slip velocity is shown by application to a straight through resonator.

2. Isentropic wave approximation theory for perforated pipes with sheared grazing mean flow

2.1. Quasi one-dimensional continuity and momentum equations

Consider a perforated hard-walled uniform pipe of cross-sectional area S. Presuming one-dimensional acoustic wave motion superimposed on a uniform parallel mean shear flow in the pipe and neglecting the viscosity effects, the conservation laws for mass and axial momentum of the fluid flow in the pipe can be expressed in a quasi-one-dimensional form as

$$S\frac{\partial \rho}{\partial t}+\frac{\partial}{\partial x}\left[\rho\int_S v\,\mathrm{d}S\right]=S\dot{\mu} \tag{1}$$

$$\frac{\partial}{\partial t}\left[\rho\int_S v\,\mathrm{d}S\right]+\frac{\partial}{\partial x}\left[\rho\int_S v^2\,\mathrm{d}S\right]+S\frac{\partial p}{\partial x}=S\dot{\mu}w \tag{2}$$

respectively, where x denotes the duct axis, t denotes the time and $\dot{\mu}$ denotes the rate of mass inflow into the pipe per unit volume of the pipe. The fluid density, $\rho=\rho_0+\rho'$, the fluid pressure, $p=p_0+p'$, and the particle velocity in the axial direction, $v=v_0+v'$, are assumed to consist of acoustic perturbations ρ', p' and v', which are superimposed on the time-averaged mean values ρ_0, p_0 and v_0, respectively, where prime ($'$) denotes a fluctuating part and the subscript '0' denotes a time-averaged mean part throughout the paper. All fluctuations are assumed to be small to first order and be functions of t and x only, characterizing a plane sound wave motion. ρ_0 and p_0 are assumed to be constant, and the mean flow velocity, v_0, is assumed to be axially uniform but allowed to have any arbitrary profile over the pipe cross-section. The source term on the right of

Eq. (1) represents the rate of mass inflow at the pipe wall, and the source term on the right of Eq. (2) represents the axial momentum convection at the pipe wall, where w denotes the axial fluid velocity at the pipe wall. w and $\dot{\mu}$ are decomposed similarly into mean and fluctuating parts as $w = w_0 + w'$ and $\dot{\mu} = \dot{\mu}_0 + \dot{\mu}'$, respectively, where the slip velocity w_0 is constant and $\dot{\mu}_0 = 0$, as only grazing mean flow is assumed to be present.

carrying out Upon the indicated integrations over the duct cross-section, Eqs. (1) and (2) become

$$\frac{\partial \rho}{\partial t} + \bar{v}\frac{\partial \rho}{\partial x} + \rho\frac{\partial \bar{v}}{\partial x} = \dot{\mu}, \tag{3}$$

$$\rho\left(\frac{\partial \bar{v}}{\partial t} + \bar{v}\frac{\partial \bar{v}}{\partial x}\right) + \frac{\partial}{\partial x}[\rho(\overline{v^2} - \bar{v}^2)] + \frac{\partial p}{\partial x} = \dot{\mu}(w - \bar{v}), \tag{4}$$

respectively. Here, and throughout the paper, an overbar denotes averaging over the duct cross-sectional area. Eqs. (3) and (4) are next expanded into mean and fluctuating parts and the products of acoustic perturbations are neglected as second-order small quantities. This usual linearization procedure yields the acoustic continuity and momentum equations as

$$\frac{\partial \rho'}{\partial t} + \bar{v}_0\frac{\partial \rho'}{\partial x} + \rho_0\frac{\partial v'}{\partial x} = \dot{\mu}', \tag{5}$$

$$\rho_0\left(\frac{\partial v'}{\partial t} + \bar{v}_0\frac{\partial v'}{\partial x}\right) + \beta\bar{v}_0^2\frac{\partial \rho'}{\partial x} + \frac{\partial p'}{\partial x} = (w_0 - \bar{v}_0)\dot{\mu}', \tag{6}$$

respectively, where

$$(1+\beta)\bar{v}_0^2 = \frac{1}{S}\int_S v_0^2 \ \mathrm{d}S, \quad \bar{v}_0 = \frac{1}{S}\int_S v_0 \ \mathrm{d}S. \tag{7}$$

The acoustic continuity equation, Eq. (5), is the same as the continuity equation of the existing theory [3–8]. The acoustic momentum equation, Eq. (6), differs from the momentum equation of the existing theory in two respects. First is the β term, which is new and accounts for the effect of the mean flow velocity profile. The second is the source term on the right, which is also new. Thus, it transpires that, the existing theory tacitly presumes that $w_0 = \bar{v}_0$, that is, the slip velocity at the pipe wall is equal to the mean flow velocity averaged over the pipe cross-section. This is a consistent condition only if the mean flow velocity profile is uniform. Therefore, it follows that, if the mean flow velocity profile is to be allowed to have an arbitrary shape, then w_0 should be left as a parameter. Introduction of this parameter, which is more conveniently considered as a fraction of $\bar{v}_0$ as $\eta = w_0/\bar{v}_0$, and the parameter β are the distinguishing features of the present theory.

2.2. Isentropic wave approximation

Eqs. (5) and (6) can be closed for the determination of ρ', p' and v' in two ways. First is to assume, as in the existing theory, that sound propagation is isentropic and use the state equation $\mathrm{d}p = c^2\mathrm{d}\rho$, or $p' = c^2\rho'$, where c denotes the speed of sound, $c^2 = \gamma p_0/\rho_0$, and γ is the ratio of specific heat coefficients. If the mean flow velocity profile is uniform, this relationship is tantamount to the energy equation. For a general mean flow velocity profile, however, the energy conservation

equation itself has to be used. Nevertheless, as it will transpire subsequently, the isentropic wave relationship provides a good approximation to the energy conservation equation. The present section describes this approximate theory, which is advocated also for its simplicity. The proper approach which uses the energy equation is deferred to Section 4.

Upon using the state equation $p' = c^2\rho'$, and assuming $\exp(-i\omega t)$ time dependence, where i denotes the unit imaginary number and ω denotes the radian frequency, Eqs. (5) and (6) can be expressed as

$$\left(\bar{M}_0 \frac{\partial}{\partial x} - ik\right)p' + \rho_0 c \frac{\partial v'}{\partial x} = \dot{\mu}' c, \tag{8}$$

$$\alpha^2 \frac{\partial p'}{\partial x} + \rho_0 c\left(\bar{M}_0 \frac{\partial}{\partial x} - ik\right)v' = -(1-\eta)\bar{M}_0 \dot{\mu}' c, \tag{9}$$

where $\bar{M}_0$ $(= \bar{v}_0/c)$ is the Mach number of the cross-section averaged mean flow velocity, k $(= \omega/c)$ is the wavenumber, η $(= w_0/\bar{v}_0)$ is the ratio of the slip velocity to the cross-section averaged mean flow velocity, and

$$\alpha^2 = 1 + \beta \bar{M}_0^2. \tag{10}$$

Upon defining effective characteristic impedance, z_e, and effective speed of sound, c_e, as

$$z_e = \frac{\rho_0 c}{\alpha}, \quad c_e = \alpha c, \tag{11}$$

Eqs. (8) and (9) can be recast as, respectively,

$$\left(\bar{M}_e \frac{\partial}{\partial x} - ik_e\right)p' + z_e \frac{\partial v'}{\partial x} = \frac{\dot{\mu}' c_e}{\alpha^2}, \tag{12}$$

$$\frac{\partial p'}{\partial x} + z_e\left(\bar{M}_e \frac{\partial}{\partial x} - ik_e\right)v' = -(1-\eta)\bar{M}_e \frac{\dot{\mu}' c_e}{\alpha^2}, \tag{13}$$

where

$$\bar{M}_e = \frac{\bar{M}_0}{\alpha}, \quad k_e = \frac{k}{\alpha}. \tag{14}$$

In the next section, the discrete method of Ref. [3] is reformulated on the basis of Eqs. (12) and (13) and applied to the experiment of Ref. [9].

3. An improved discrete method for perforation with grazing mean flow

3.1. Wave transfer across a row of perforate holes

In the discrete method of Ref. [3], a perforation is modeled as an axial distribution of rows of compact holes drilled on the pipe wall. The wave transfer relationship across a number of rows is calculated by combining the wave transfer relation across the discontinuity created by each row of holes with transfer matrices of the solid pipe sections separating those rows. The latter are given

by the solution of the homogeneous forms of Eqs. (12) and (13) and conveniently expressed in terms of the acoustic pressure wave components p^+ and p^- as [11]

$$p^+(x) = p^+(0)\exp\left(\frac{\mathrm{i}k_e x}{1+\bar{M}_e}\right), \tag{15}$$

$$p^-(x) = p^-(0)\exp\left(\frac{-\mathrm{i}k_e x}{1-\bar{M}_e}\right), \tag{16}$$

where

$$p'(x) = p^+(x) + p^-(x), \quad z_e v'(x) = p^+(x) - p^-(x), \tag{17}$$

and the superscripts '+' and '−' refer to waves traveling in forward ($+x$) and backward directions.

The sound wave transfer across a row of holes, on the other hand, is determined by the solution of Eqs. (12) and (13). To obtain this solution, consider a perforate row at $x=\xi$. Since the holes are assumed to be compact, the fluctuating part of the rate of mass inflow at this plane per unit volume of the pipe can be expressed as

$$\dot{\mu}'(x) = m'(x)\delta(x-\xi)/S, \tag{18}$$

where S denotes the pipe cross-sectional area, $\delta(x)$ denotes a Dirac function located at $x=0$ and $m'(x)$ denotes the fluctuating part of the rate of mass inflow. It is convenient to express the latter as $m'(x)=\rho_0 Q(x)$, where $Q(x)$ denotes the fluctuating part of the rate of volume flow into the pipe.

Upon substituting Eq. (18) and integrating across the region $x=\xi$, Eqs. (12) and (13) give the required jump relations across the perforate row at $x=\xi$:

$$\bar{M}_e\left[p'(\xi_+) - p'(\xi_-)\right] + z_e\left[v'(\xi_+) - v'(\xi_-)\right] = \frac{z_e Q(\xi)}{S}, \tag{19}$$

$$\left[p'(\xi_+) - p'(\xi_-)\right] + z_e\bar{M}_e\left[v'(\xi_+) - v'(\xi_-)\right] = -(1-\eta)\bar{M}_e\frac{z_e Q(\xi)}{S}, \tag{20}$$

or, in matrix notation

$$\begin{bmatrix} p'(\xi_+) \\ z_e v'(\xi_+) \end{bmatrix} = \begin{bmatrix} p'(\xi_-) \\ z_e v(\xi_-) \end{bmatrix} + \begin{bmatrix} -(2-\eta)\bar{M}_e \\ 1+(1-\eta)\bar{M}_e^2 \end{bmatrix}\frac{z_e Q(\xi)}{S(1-\bar{M}_e^2)}, \tag{21}$$

where the subscripts '+' and '−' denote the planes just downstream and just upstream of $x=\xi$.

Alternatively, by using the decomposition of Eq. (17), Eq. (21) can be re-cast in terms of the pressure wave components p^+ and p^- as

$$\begin{bmatrix} p^+(\xi_+) \\ \\ p^-(\xi_+) \end{bmatrix} = \begin{bmatrix} p^+(\xi_-) \\ \\ p^-(\xi_-) \end{bmatrix} + \frac{z_e Q(\xi)}{2S}\begin{bmatrix} \frac{1-(1-\eta)\bar{M}_e}{1+\bar{M}_e} \\ \\ -\frac{1+(1-\eta)\bar{M}_e}{1-\bar{M}_e} \end{bmatrix}. \tag{22}$$

This relationship corresponds to Eq. (2) of Ref. [3] where it was derived under the tacit assumptions of $\beta=0$ and $\eta=1$, and implemented by applying a heuristic compact correction, ε, to ξ_+ and ξ_- as $\xi_+=\xi+\varepsilon$ and $\xi_-=\xi-\varepsilon$. Before showing the modifications which Eq. (22) implies for the

discrete method of Ref. [3], it is expedient to apply it to the experiment of Ref. [9], which apparently reports the failure of the segmentation method [1], as well as the discrete method of Ref. [3].

3.2. The experiment of Aurégan and Leroux [9]

Measured in this experiment are the elements of the plane sound wave transfer matrix across a row of perforate holes backed up by a cavity. Eq. (21) can be transformed to the form of the measured wave transfer relationship by introducing the combined impedance, $z(\xi)$, of a perforate row at $x=\xi$ and its backing cavity

$$z(\xi)=\frac{p'(\xi_-)}{U(\xi)},\quad U(\xi)=\frac{Q(\xi)}{A}, \tag{23}$$

where U denotes the radial fluid velocity at the interface between the holes and the pipe wall and A denotes the total open area of the row. Upon introducing Eq. (23), Eq. (21) can be expressed as

$$\begin{bmatrix} p'(\xi_+) \\ z_e v'(\xi_+) \end{bmatrix} = \begin{bmatrix} 1-(2-\eta)\bar{M}_e C_p & 0 \\ [1+(1-\eta)\bar{M}_e^2]C_p & 1 \end{bmatrix} \begin{bmatrix} p'(\xi_-) \\ z_e v'(\xi_-) \end{bmatrix}. \tag{24}$$

Here

$$C_p=\frac{z_e}{z(\xi)}\frac{A}{S}\frac{1}{1-\bar{M}_e^2}=\frac{Y_s(\xi)}{1-\bar{M}_e^2}. \tag{25}$$

Aurégan and Leroux [9] have found that their experimental data fits very accurately to the relationship

$$\begin{bmatrix} p'(\xi_+) \\ \rho_0 c v'(\xi_+) \end{bmatrix} = \begin{bmatrix} 1-1.5\bar{M}_0 C_p & 0 \\ C_p & 1 \end{bmatrix} \begin{bmatrix} p'(\xi_-) \\ \rho_0 c v'(\xi_-) \end{bmatrix}, \tag{26}$$

and, having calculated the corresponding prediction of Sullivan's segmentation method [1] as

$$\begin{bmatrix} p'(\xi_+) \\ \rho_0 c v'(\xi_+) \end{bmatrix} = \begin{bmatrix} 1-\bar{M}_0 C_p & \bar{M}_0^2 C_p \\ C_p & 1+\bar{M}_0 C_p \end{bmatrix} \begin{bmatrix} p'(\xi_-) \\ \rho_0 c v'(\xi_-) \end{bmatrix}, \tag{27}$$

have concluded that the segmentation method fails in providing an accurate representation of the plane wave transmission across a perforate row. The authors tend to present this result as equally valid also for the discrete method of Ref. [3]. This is not true, as the latter method yields not Eq. (27) but the relationship

$$\begin{bmatrix} p'(\xi_+) \\ \rho_0 c v'(\xi_+) \end{bmatrix} = \begin{bmatrix} 1-\bar{M}_0 C_p & 0 \\ C_p & 1 \end{bmatrix} \begin{bmatrix} p'(\xi_-) \\ \rho_0 c v'(\xi_-) \end{bmatrix}, \tag{28}$$

which is the same as the measured transfer relationship (26) except for the factor 1.5. Eq. (28) is Eq. (24) for $\beta=0$ and $\eta=1$. For $\eta=0.5$, Eq. (24) becomes

$$\begin{bmatrix} p'(\xi_+) \\ z_e v'(\xi_+) \end{bmatrix} = \begin{bmatrix} 1-1.5\bar{M}_e C_p & 0 \\ (1+0.5\bar{M}_e^2)C_p & 1 \end{bmatrix} \begin{bmatrix} p'(\xi_-) \\ z_e v'(\xi_-) \end{bmatrix}, \tag{29}$$

which is practically the same as the measured transfer relationship, as the mean flow Mach number in the experiment of Ref. [9] was $\bar{M}_0 = 0.143$. For a mean flow Mach number of this order, $\alpha = 1$ with much less than 1% error, as β is much less than unity for the likely mean flow velocity profiles (see Section 4.2). Consequently, Eq. (29) represents the measured transfer relationship (26) with much less than 1% error. Thus, it is seen that, whilst the claim of Ref. [9] regarding the failure of the segmentation method [1] appears to be true, this is not a general rule for the discrete approach. The discrete method of Ref. [3] already provided a close representation of the empirical wave transfer relationship, and the present extension of this method can predict it almost exactly for $\eta = 0.5$.

The improved counterparts of Eqs. (21) and (22) that are based on the energy equation proper are given in Section 4.

3.3. Modeling of muffler elements with parallel perforated pipes

Presented in this section is a revision of the discrete method of Ref. [3] for sound transmission across a pack of multiple parallel perforated pipes that are enclosed in a solid pipe or casing. In this method it suffices to derive a wave transfer relationship for a pack in which the perforated pipes all have a perforate row at the same axial position, as shown in Fig. 1. The derivation of this transfer relation in the absence of the mean flow profile effects considered here but with perforate holes generalized to the concept of compact acoustic devices is given in some detail in Ref. [3].

Essentially, the revision entails the use of Eq. (22) in place of Eq. (2) of Ref. [3], which is Eq. (22) with $\beta = 0$ and $\eta = 1$. Therefore, to inject the mean flow profile effects into the discrete method, it suffices to redefine the vector $\mathbf{B}_j$ in Eq. (9) of Ref. [3] as

$$\mathbf{B}_j = \frac{1}{\alpha_j}\begin{bmatrix} [1-(1-\eta_j)\bar{M}_{ej}](1+\bar{M}_{ej})^{-1} \\ -[1+(1-\eta_j)\bar{M}_{ej}](1-\bar{M}_{ej})^{-1} \end{bmatrix}, \tag{30}$$

where the subscript j, $j = 1, 2\ldots$, denotes the pipe number, pipe 1 being the enclosing pipe. Accordingly, the matrix $\mathbf{M}_j$ defined by Eq. (23) of Ref. [3] for the two-pipe case should be

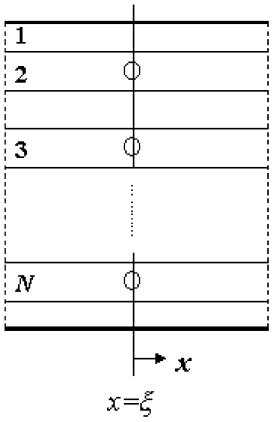

Fig. 1. Multiple parallel perforate rows.

expressed now as

$$\mathbf{M}_j = \frac{1}{\alpha_j}\begin{bmatrix} [1-(1-\eta_j)\bar{M}_{ej}](1+\bar{M}_{ej})^{-1} & [1-(1-\eta_j)\bar{M}_{ej}](1+\bar{M}_{ej})^{-1} \\ -[1+(1-\eta_j)\bar{M}_{ej}](1-\bar{M}_{ej})^{-1} & -[1+(1-\eta_j)\bar{M}_{ej}](1-\bar{M}_{ej})^{-1} \end{bmatrix}, \quad j=1,2. \tag{31}$$

The rest of the formulation of Ref. [3] applies as is.

4. The proper form of the theory for perforated pipes with sheared grazing mean flow

4.1. A quasi-one-dimensional energy equation

Now consider the use of the energy equation to close Eqs. (5) and (6). Again, presuming one-dimensional acoustic wave motion superimposed on a parallel uniform mean shear flow in the pipe and neglecting the visco-thermal effects, but allowing for an arbitrary mean flow velocity profile over the pipe cross-section, the energy equation can be expressed in quasi-one-dimensional form as

$$\frac{\partial}{\partial t}\left[\rho\int_S e\,\mathrm{d}S\right] + \frac{\partial}{\partial x}\left[\rho\int_S h^0 v\,\mathrm{d}S\right] = S\dot{\mu}h_w^0, \tag{32}$$

where

$$e = u + \tfrac{1}{2}v^2, \quad h^0 = e + \frac{p}{\rho}. \tag{33}$$

Here, e, u and h^0 denote, respectively, the specific total energy, the specific internal energy and the specific stagnation enthalpy of the fluid, and h_w^0 denotes the specific stagnation enthalpy carried by the mass flow at the pipe wall. The objective of the subsequent analysis is to transform Eq. (32) into a form that gives, upon linearization, an equation that closes Eqs. (5) and (6) for the determination of ρ', p' and v'.

Upon carrying out the indicated integrations over the duct cross-section, Eq. (32) can be written as

$$\frac{\partial}{\partial t}\left[\rho\{\bar{e} + \tfrac{1}{2}(\overline{v^2} - \bar{v}^2)\}\right] + \frac{\partial}{\partial x}\left[\rho\bar{v}\left\{\bar{h}^0 + \tfrac{1}{2}\left(\frac{\overline{v^3}}{\bar{v}} - \bar{v}^2\right)\right\}\right] = \dot{\mu}h_w^0, \tag{34}$$

where

$$\bar{e} = u + \tfrac{1}{2}\bar{v}^2, \quad \bar{h}^0 = \bar{e} + \frac{p}{\rho}. \tag{35}$$

When Eqs. (3) and (4) are substituted, Eq. (34) simplifies to

$$\rho\left(\frac{\partial u}{\partial t} + \bar{v}\frac{\partial u}{\partial x}\right) - \bar{v}\frac{\partial}{\partial x}[\rho(\overline{v^2} - \bar{v}^2)] + p\frac{\partial \bar{v}}{\partial x} = \dot{\mu}\left[h_w^0 - \bar{v}(w - \bar{v}) - \bar{e}\right], \tag{36}$$

which, upon using the perfect gas state equation $(\gamma-1)\rho \mathrm{d}u = \mathrm{d}\rho - (p/\rho)\mathrm{d}\rho$, can be expressed as

$$\frac{\partial p}{\partial t} + \bar{v}\frac{\partial p}{\partial x} + \gamma p \frac{\partial \bar{v}}{\partial x} + \tfrac{1}{2}(\gamma-1)\left[\frac{\partial}{\partial t}[\rho(\overline{v^2} - \bar{v}^2)] + \frac{\partial}{\partial x}[\rho(\overline{v^3} - \bar{v}^3)] - 2\bar{v}\frac{\partial}{\partial x}[\rho(\overline{v^2} - \bar{v}^2)]\right] = \dot{\mu}(\gamma-1)\left[\tfrac{1}{2}(w-\bar{v})^2 + \frac{c^2}{\gamma-1}\right]. \tag{37}$$

This equation can be linearized as usual by partitioning into mean and fluctuating parts, assuming the mean part is satisfied by the mean flow and neglecting the products of acoustic perturbations as second order small quantities. This process yields for the acoustic fluctuations

$$\frac{\partial p'}{\partial t} + \bar{v}_0\frac{\partial p'}{\partial x} + \left[\gamma p_0 + \rho_0(\gamma-1)\beta\bar{v}_0^2\right]\frac{\partial v'}{\partial x} + \tfrac{1}{2}(\gamma-1)(\chi-3\beta)\bar{v}_0^3\frac{\partial \rho'}{\partial x} = \dot{\mu}'\left[c^2 + \tfrac{1}{2}(\gamma-1)\left[(\eta-1)^2 - \beta\right]\bar{v}_0^2\right], \tag{38}$$

where

$$(1+\chi)\bar{v}_0^3 = \frac{1}{S}\int_S v_0^3 \,\mathrm{d}S. \tag{39}$$

Thus, the consideration of the energy equation introduces a new parameter, χ, into the analysis. For $\eta = 1$, $\beta = 0$ and $\chi = 0$, the energy equation (38) becomes a statement of isentropic propagation $p' = c^2\rho'$, which is readily verified from Eqs. (38) and (5).

4.2. Further improvement of the discrete method for perforation with grazing mean flow

Upon substituting Eq. (18) in Eqs. (5), (6) and (38) and integrating the resulting equations across a perforate row at $x = \xi$, the following jump equations are obtained:

$$\begin{bmatrix} p'(\xi_+) \\ \rho_0 c v'(\xi_+) \\ c^2\rho'(\xi_+) \end{bmatrix} = \begin{bmatrix} p'(\xi_-) \\ \rho_0 c v'(\xi_-) \\ c^2\rho'(\xi_-) \end{bmatrix} + \begin{bmatrix} b_1 \\ b_2 \\ b_3 \end{bmatrix} \frac{\rho_0 c Q(\xi)}{S(1-\bar{M}_0^2)}, \tag{40}$$

where

$$b_1 = b\left[\tfrac{1}{2}(\gamma-1)\{(2-\eta)(\chi-3\beta) - 3\beta^2 + \beta\eta^2 - (1-\eta)^2\}\bar{M}_0^2 - 2 + \eta\right]\bar{M}_0, \tag{41}$$

$$b_2 = b\left[1 + \left[\tfrac{1}{2}(\gamma-1)\{2\beta - \chi + (1-\eta)^2\} + \beta + 1 - \eta\right]\bar{M}_0^2\right], \tag{42}$$

$$b_3 = b\left[\tfrac{1}{2}(\gamma-1)\{3\beta - (1-\eta)^2\} - 2 + \eta\right]\bar{M}_0, \tag{43}$$

$$b = \frac{1-\bar{M}_0^2}{1 + \left\{\tfrac{1}{2}(\gamma-1)(5\beta-\chi) + \beta - 1\right\}\bar{M}_0^2}. \tag{44}$$

Eq. (40) is the energy equation based counterpart of Eq. (21). It is noteworthy that Eq. (21) can be recovered from Eq. (40) by taking $\gamma = 1$. The contribution of the correct γ is in general small, as the mean flow velocity profile parameters β and χ are much less than unity for likely

profiles. The '$1/n$'th power law turbulent flow profile may be used to obtain an idea about the likely values of the parameters β and χ, as, for sufficiently large n, this law provides an approximate representation of slip flow with a flat core. Thus, assuming that the actual mean flow velocity profiles can be approximated for $n \geqslant 5$, possible estimates for β and χ can be stated as $\beta < 0.04$ and $\chi < 0.1$, and the transfer matrix of the experiment of Ref. [9] can be expressed as

$$\begin{bmatrix} p'(\xi_+) \\ \rho_0 c v'(\xi_+) \end{bmatrix} = \begin{bmatrix} 1 - [(2-\eta)\bar{M}_0 + O[\bar{M}_0^3]]C_p & 0 \\ [1 + (1-\eta)(3-2\eta)\bar{M}_0^2 + O[\bar{M}_0^4]]C_p & 1 \end{bmatrix} \begin{bmatrix} p'(\xi_-) \\ \rho_0 c v'(\xi_-) \end{bmatrix}, \tag{45}$$

where increasing n only effects the indicated higher order terms. It is seen that, for subsonic low Mach numbers, Eq. (45) is almost identical to its counterpart, Eq. (24), which is based on the isentropic wave assumption. Hence, in general, the isentropic relationship $p' = c^2\rho'$ provides a good approximate representation of the energy equation for subsonic low Mach number mean flows.

5. An improved distributed parameter method for multiple perforated pipe muffler elements with grazing mean flow

The existing distributed parameter method [4–8] for acoustic analysis of perforated multiple pipe mufflers with grazing mean flow is based on Eqs. (12) and (13) with $\eta = 1$ and $\beta = 0$. Presented in this section is an extension of this method for any η and β for the grazing mean flow case. Both, parallel and co-axial multiple perforated pipe arrangements are considered. The distributed parameter method can also be formulated by the proper approach in which the energy equation (38) is used to close Eqs. (5) and (6), however, this formulation is not considered, as it is rather cumbersome and is implemented much more easily by the discrete approach shown in Section 4. Furthermore, for subsonic mean flow Mach numbers, Eqs. (12) and (13) are sufficiently accurate.

5.1. Parallel multiple perforated pipes

Consider an arbitrary number of parallel perforated pipes enclosed in a solid pipe or casing, which communicate with each other over a common perforate length L. The pipes are numbered consecutively as pipe 1,2,…, pipe 1 being the enclosing casing, as shown in Fig. 2a. The problem is to derive a plane sound wave transfer relationship between the ends of the pipes. The solution of this problem is considered in some detail in Ref. [7] and, therefore, here it suffices to present only the salient modifications arising from the introduction of the parameters η and β into the analysis. The notation of Ref. [7] is followed as much as possible for ease of reference.

When applied to pipes 1,2,…, Eqs. (12) and (13) can be expressed in matrix form as [7]

$$\frac{\partial \mathbf{Q}}{\partial x} = \mathbf{U}\mathbf{Q}(x), \tag{46}$$

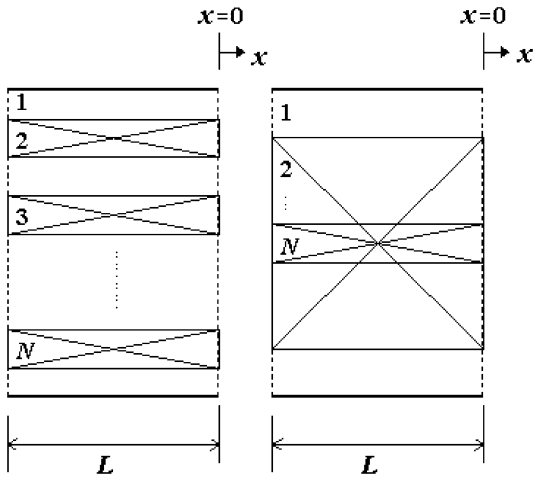

Fig. 2. Multiple perforated pipe elements: (a) parallel element (left); (b) co-axial element (right).

which is a concise representation of

$$\frac{\partial}{\partial x}\begin{bmatrix}\mathbf{Q}_1(x)\\ \mathbf{Q}_2(x)\\ \vdots\end{bmatrix} = -\begin{bmatrix}\mathbf{M}_1\mathbf{B}_{11} & \mathbf{M}_1\mathbf{B}_{12} & \cdots\\ \mathbf{M}_2\mathbf{B}_{21} & \mathbf{M}_2\mathbf{B}_{22} & \cdots\\ \vdots & \vdots & \ddots\end{bmatrix}\begin{bmatrix}\mathbf{Q}_1(x)\\ \mathbf{Q}_2(x)\\ \vdots\end{bmatrix}, \tag{47}$$

where

$$\mathbf{Q}_j(x) = \begin{bmatrix}p_j'(x)\\ z_{ej}v_j'\end{bmatrix}, \quad j = 1,2,\ldots, \tag{48}$$

$$\mathbf{M}_j = \frac{1}{1-\bar{M}_{ej}^2}\begin{bmatrix}1 & -\bar{M}_{ej}\\ -\bar{M}_{ej} & 1\end{bmatrix}, \quad j = 1,2,\ldots, \tag{49}$$

$$\mathbf{B}_{jj} = \begin{bmatrix}-(1-\eta_j)\bar{M}_{ej}a_j & -\mathrm{i}k_{ej}\\ -\mathrm{i}k_{ej}+a_j & 0\end{bmatrix}, \quad j = 1,2,\ldots, \tag{50}$$

$$\mathbf{B}_{j1} = \begin{bmatrix}(1-\eta_j)\bar{M}_{ej}a_j & 0\\ -a_j & 0\end{bmatrix}, \quad j = 2,3,\ldots, \tag{51}$$

$$\mathbf{B}_{1j} = \begin{bmatrix}(1-\eta_1)\bar{M}_{e1}b_j & 0\\ -b_j & 0\end{bmatrix}, \quad j = 2,3,\ldots, \tag{52}$$

and the remaining 2×2 blocks of matrix $\mathbf{B}$ are zero. In the foregoing equations, the subscript 'j' denotes the pipe numbers, and the parameters a_j and b_j are defined as

$$\begin{gathered} a_j = \frac{2\sigma_j}{\alpha_j r_j \varsigma_j}, \quad b_j = \frac{\alpha_j S_j}{\alpha_1 S_1} a_j, \quad j = 2, 3, \ldots \\ a_1 = b_2 + b_3 + \cdots, \quad (1 - \eta_1) a_1 = (1 - \eta_{1,2}) b_2 + (1 - \eta_{1,3}) b_3 + \cdots, \end{gathered} \tag{53}$$

where S_j, σ_j, r_j and ζ_j denote, respectively, the cross-sectional area, the porosity, the hydraulic radius and the perforate impedance of pipe j, and $\eta_{1,j}$ denotes the slip velocity ratio, for the mean flow in pipe 1, on the outer surface of pipe j.

The solution of Eq. (46) over the perforate length L can be expressed as

$$\mathbf{Q}(L) = \mathbf{\Psi}^{-1} \begin{bmatrix} e^{\lambda_1 x} & 0 & \cdots \\ 0 & e^{\lambda_2 x} & \cdots \\ \vdots & \vdots & \ddots \end{bmatrix} \mathbf{\Psi} \mathbf{Q}(0), \tag{54}$$

since matrix $\mathbf{U}$ has constant elements. Here, λ_j, $j = 1,2,\ldots$, denote the eigenvalues of matrix $\mathbf{U}$ in ascending order and $\mathbf{\Psi}$ is the modal matrix whose columns are the corresponding right eigenvectors.

Eq. (54) is the required wave transfer relation across a pack of arbitrary number of coupled parallel perforated pipes in impedance matrix form. It can be re-cast in a scattering matrix form by using the decomposition of Eq. (17), which is expressed now in matrix notation as

$$\mathbf{Q}_j(x) = \mathbf{E}_j \mathbf{P}_j(x), \tag{55}$$

where

$$\mathbf{P}_j(x) = \begin{bmatrix} p_j^+(x) \\ p_j^-(x) \end{bmatrix}, \quad \mathbf{E}_j = \begin{bmatrix} 1 & 1 \\ 1 & -1 \end{bmatrix}. \tag{56}$$

Upon applying this transformation, Eq. (46) can be expressed as

$$\frac{\partial}{\partial x} \begin{bmatrix} \mathbf{P}_1(x) \\ \mathbf{P}_2(x) \\ \vdots \end{bmatrix} = -\frac{1}{2} \begin{bmatrix} \mathbf{E}_1 \mathbf{M}_1 \mathbf{B}_{11} \mathbf{E}_1 & \mathbf{E}_1 \mathbf{M}_1 \mathbf{B}_{12} \mathbf{E}_2 & \cdots \\ \mathbf{E}_2 \mathbf{M}_2 \mathbf{B}_{21} \mathbf{E}_1 & \mathbf{E}_2 \mathbf{M}_2 \mathbf{B}_{22} \mathbf{E}_2 & \cdots \\ \vdots & \vdots & \ddots \end{bmatrix} \begin{bmatrix} \mathbf{P}_1(x) \\ \mathbf{P}_2(x) \\ \vdots \end{bmatrix}, \tag{57}$$

or, briefly,

$$\frac{\partial \mathbf{P}}{\partial x} = \mathbf{H} \mathbf{P}(x), \tag{58}$$

solution of which gives the required scattering matrix relationship as

$$\mathbf{P}(L) = \mathbf{\Phi}^{-1} \begin{bmatrix} e^{\lambda_1 x} & 0 & \cdots \\ 0 & e^{\lambda_2 x} & \cdots \\ \vdots & \vdots & \ddots \end{bmatrix} \mathbf{\Phi} \mathbf{P}(0), \tag{59}$$

since matrices **H** and **U** have identical eigenvalues. It can be shown that the eigenvectors of these matrices are related by $\mathbf{\Phi} = \mathbf{\Psi E}$, where **E** denotes the block diagonal matrix having matrices $\boldsymbol{E}_j, j = 1, 2, \ldots$, as its diagonal blocks.

5.2. Coaxial multiple perforated pipes

Consider an arbitrary number of coaxial perforated pipes enclosed in a solid pipe or casing, which communicate with each other over a common perforate length L. The pipes are numbered from the outer to the inner pipe, consecutively as pipe 1, 2,…,N, as shown in Fig. 2b, pipe 1 being the enclosing casing and pipe N the innermost pipe.. The problem is to derive a plane sound wave transfer relationship between the ends of the pipes. The solution of this problem is considered in some detail in Ref. [12]. It can be shown that, except for the definition of matrix **B**, the solution represented by Eq. (59) is formally valid for this case, too, provided that matrix **B** is defined now as

$$\mathbf{B}_{jj} = \begin{bmatrix} -(1-\eta_{j,j+1})\bar{M}_{ej}b_{j+1} - (1-\eta_j)\bar{M}_{ej}a_j & -\mathrm{i}k_{ej} \\ -\mathrm{i}k_{ej} + a_j + b_{j+1} & 0 \end{bmatrix}, \quad j = 1, 2, \ldots, N, \tag{60}$$

$$\mathbf{B}_{j,j+1} = \begin{bmatrix} (1-\eta_{j,j+1})\bar{M}_{ej}b_{j+1} & 0 \\ -b_{j+1} & 0 \end{bmatrix}, \quad j = 1, 2, \ldots, N-1, \tag{61}$$

$$\mathbf{B}_{j+1,j} = \begin{bmatrix} (1-\eta_j)\bar{M}_{ej}a_j & 0 \\ -a_j & 0 \end{bmatrix}, \quad j = 2, 3, ..., N, \tag{62}$$

and the remaining 2×2 blocks of matrix **B** are zero. Here, the subscript 'j' denotes the pipe numbers, η_j denotes the slip velocity ratio on the inner surface of the outer wall of pipe j, $\eta_{j,j+1}$ denotes the slip velocity ratio, for the mean flow in pipe j, on the on the outer surface of pipe $j+1$, and the parameters a_j and b_j are defined as

$$a_j = \frac{2\sigma_j P_j}{\alpha_j S_j \zeta_j}, \quad b_{j+1} = \frac{\alpha_{j+1} S_{j+1}}{\alpha_j S_j} a_{j+1}, \quad a_1 = b_{N+1} = 0, \tag{63}$$

where N denotes the number of pipes, S_j is the cross-sectional area of the annular space between pipe j and pipe $j+1$, $j = 1, 2, \ldots, N-1$, S_N being the cross-sectional area of the innermost pipe, pipe 1 and P_j, σ_j, and ζ_j are, respectively, the perimeter, the porosity and the hole impedance of the outer wall of pipe j. The enclosing casing, pipe 1, is assumed to be solid. Then, its porosity is zero, $\sigma_1 = 0$, and, therefore, $a_1 = 0$. By definition: $S_{N+1} = 0$ and, hence, $b_{N+1} = 0$.

5.3. Application to a straight-through resonator

Although the present theory is currently validated only in the context of the experimental data of Ref. [9], it may be of interest to show the effect of the new parameters β and η on sound attenuation of a typical practical perforated pipe muffler element. A well-known muffler employing a perforated pipe is the straight-through resonator, shown in Fig. 3, which is the $N = 2$ case of Fig. 2a or b with pipe 1 having rigid closed ends. A well-studied geometry of this with

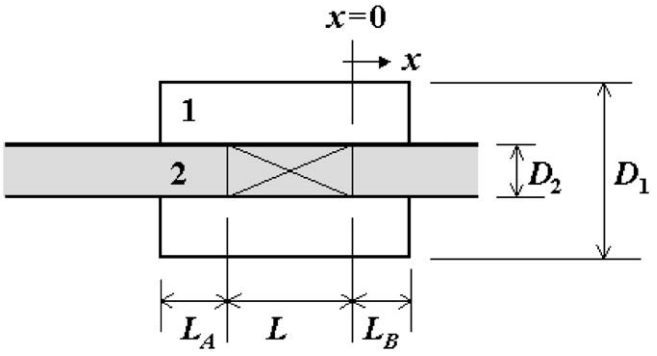

Fig. 3. Straight-through resonator: $L=325$ mm, $L_A=175$ mm, $L_B=100$ mm, $D_1=250$ mm, $D_2=75$ mm.

mean flow [6] consists of a 600 mm long and 250 mm diameter casing having rigid end-caps and a co-axial 75 mm diameter pipe of wall thickness 1.5 mm, the portion of which that is within the casing being uniformly perforated with circular holes of diameter 3 mm over a length of 325 mm, with 175 and 100 mm long inlet and outlet side-branches, respectively. For this muffler element, Eq. (59) is written as

$$\begin{bmatrix} \mathbf{P}_1(L) \\ \mathbf{P}_2(L) \end{bmatrix} = \begin{bmatrix} \mathbf{T}_{11} & \mathbf{T}_{12} \\ \mathbf{T}_{21} & \mathbf{T}_{22} \end{bmatrix} \begin{bmatrix} \mathbf{P}_1(0) \\ \mathbf{P}_2(0) \end{bmatrix}, \tag{64}$$

which, upon introducing end-cap boundary conditions, can be expressed as

$$\mathbf{P}_2(L) = \mathbf{T}_{2,0}\mathbf{P}_2(0), \tag{65}$$

where the transfer matrix $\mathbf{T}_{2,0}$ is

$$\mathbf{T}_{2,0} = \left[\mathbf{T}_{22} - \frac{\mathbf{T}_{21} \begin{bmatrix} 1 & -r_1(L) \\ r_1(0) & -r_1(0)r_1(L) \end{bmatrix} \mathbf{T}_{12}}{\begin{bmatrix} 1 & -r_1(L) \end{bmatrix} \mathbf{T}_{11} \begin{bmatrix} 1 \\ r_1(0) \end{bmatrix}} \right]. \tag{66}$$

Here, $r_1(x)$ denotes the reflection coefficient at plane x of pipe 1. For the case of rigid end-caps, $r_1(0)=\exp(\mathrm{i}2kL_B)$ and $r_1(L)=\exp(-\mathrm{i}2kL_A)$. Hence, assuming pipe 2 has an anechoic outlet, the transmission loss of the element can be calculated from

$$TL = 20\log\left|(\mathbf{T}_{2,0})_{11}\right| \ \mathrm{d}B. \tag{67}$$

The present results for the transmission loss of this resonator for $\beta_2=0$ and $\eta_2=1$ can be compared directly with the corresponding results of Ref. [6], as the same lumped hole impedance model is used in the calculations, that is,

$$\zeta_2 = \sqrt{8\nu\omega}(1+t_2/d_2)/c + 0.3\bar{M}_{02} - \mathrm{i}k(t_2+0.25d_2), \tag{68}$$

where ν denotes the kinematic viscosity of the fluid, t and d denote the pipe wall thickness and perforate hole diameter, respectively, and the subscript '2' refers to pipe 2.

The mean flow Mach number $\bar{M}_{02}$ is varied in the range 0.1 to 0.3, which is the typical range in automotive applications. In this range of mean flow Mach numbers, the variation of parameter β_2 in its expected range of values, which is less than 0.1 or so, has no discernible effect on the transmission loss of the resonator. The results to be presented were computed for $\beta_2 = 0.01$.

Shown in Figs. 4–6 are the transmission loss characteristics of the resonator for $\bar{M}_{02} = 0.1$, 0.2 and 0.3, respectively, for perforate porosity of $\sigma_2 = 0.05$, each figure giving the characteristics for

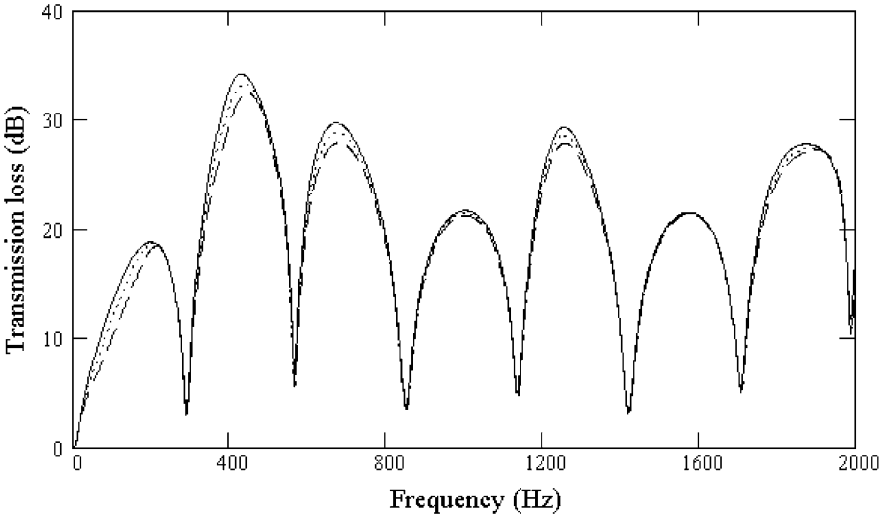

Fig. 4. Effect of slip velocity on transmission loss of the straight-through resonator: $\sigma_2 = 0.05$, $\beta_2 = 0.01$, $\bar{M}_0 = 0.1$; – – –, $\eta_2 = 0$; - - -, $\eta_2 = 0.5$; ——, $\eta_2 = 1$.

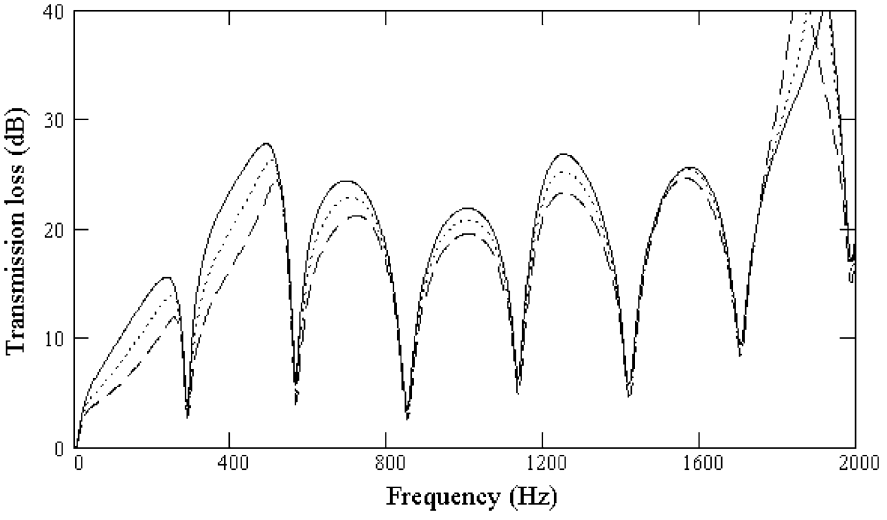

Fig. 5. Effect of slip velocity on transmission loss of the straight-through resonator: $\sigma_2 = 0.05$, $\beta_2 = 0.01$, $\bar{M}_0 = 0.2$; – – –, $\eta_2 = 0$; - - - -, $\eta_2 = 0.5$; ——, $\eta_2 = 1$.

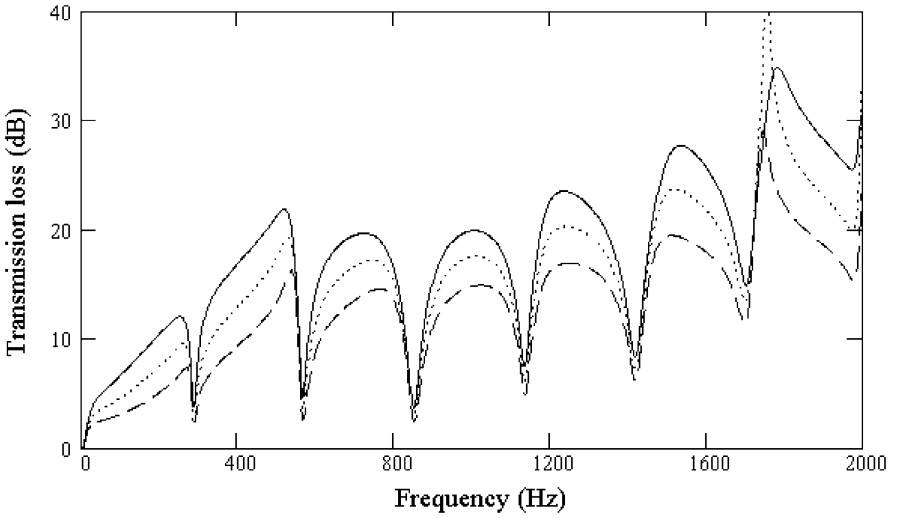

Fig. 6. Effect of slip velocity on transmission loss of the straight-through resonator: $\sigma_2=0.05$, $\beta_2=0.01$, $\bar{M}_0=0.3$; – – –, $\eta_2=0$; - - -, $\eta_2=0.5$; ——, $\eta_2=1$.

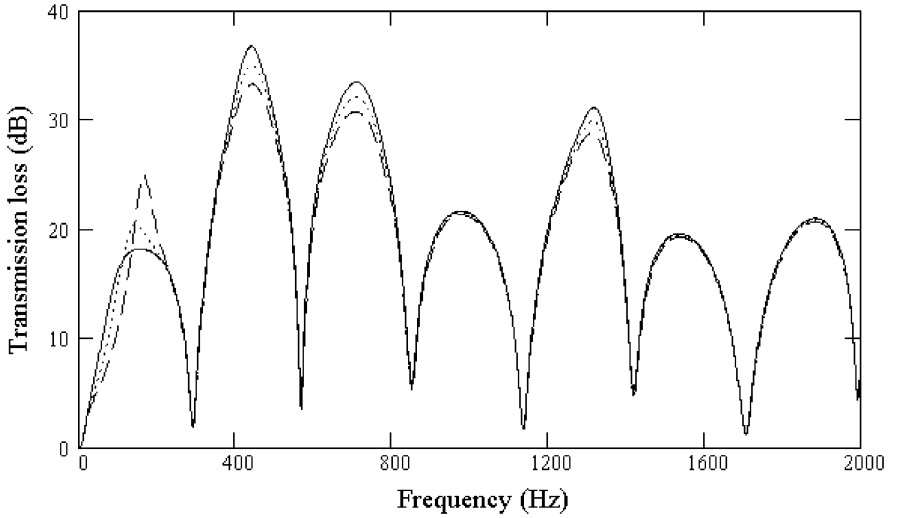

Fig. 7. Effect of slip velocity on transmission loss of the straight-through resonator: $\sigma_2=0.15$, $\beta_2=0.01$, $\bar{M}_0=0.1$; – – – $\eta_2=0$; - - -, $\eta_2=0.5$; ——, $\eta_2=1$.

three values of the slip velocity parameter, that is, for $\eta_2=0$, 0.5 and 1. The characteristics for $\eta_2=1$ in Figs. 4 and 6 are same as those of Ref. [6], which checks the accuracy of the present calculations. For the case $\bar{M}_{02}=0.1$, the slip velocity parameter has only slight effect on the transmission loss, however, as the mean flow Mach number increases, the effect of η_2 on the characteristics becomes increasingly significant.

Shown in Figs. 7–9 are the transmission loss characteristics for the same resonator but for a perforate of porosity $\sigma_2=0.15$. Again, it is observed that, the effect of slip velocity parameter tends to be more significant as the mean flow Mach numbers increases.

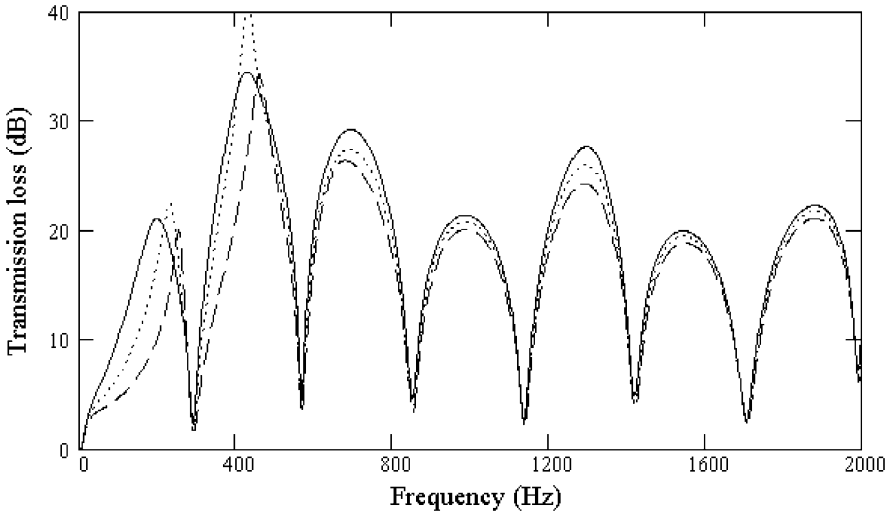

Fig. 8. Effect of slip velocity on transmission loss of the straight-through resonator: $\sigma_2 = 0.15$, $\beta_2 = 0.01$, $\bar{M}_0 = 0.2$; – – –, $\eta_2 = 0$; - - -, $\eta_2 = 0.5$; ——, $\eta_2 = 1$.

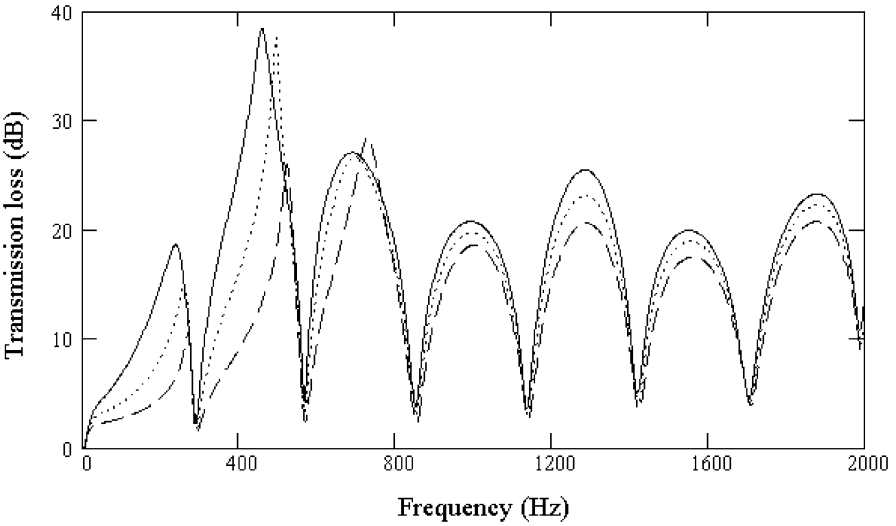

Fig. 9. Effect of slip velocity on transmission loss of the straight-through resonator: $\sigma_2 = 0.15$, $\beta_2 = 0.01$, $\bar{M}_0 = 0.3$; – – –, $\eta_2 = 0$; - - -, $\eta_2 = 0.5$; ——, $\eta_2 = 1$.

6. Conclusion

A quasi-one-dimensional theory of sound transmission in perforated pipes carrying a grazing uniform parallel shear flow is presented for the first time, and applied for the improvement of the previously published discrete and distributed parameter methods for multiple parallel and coaxial perforated pipe muffler elements. The approximate form of the theory, which assumes isentropic

wave propagation, is simpler and provides a good approximation to the proper theory for subsonic low mean flow velocity Mach numbers.

In essence, the proposed theory is distinguished from the existing theory [3–8], in which mean flow is assumed to be uniform, by the inclusion of the effect of the mean flow velocity profile in the sense of cross-sectional average, and the introduction of the slip flow at the perforate wall. For subsonic low mean flow Mach numbers, the effect of the mean flow profile is not discernible; however, the slip velocity parameter appears to have substantial effect on acoustic transmission characteristics.

At present, the proposed theory is validated only in the context of the experimental data of Ref. [9]. Further measurements are required for the validation of the theory outside this context.

References

[1] J.W. Sullivan, A method for modeling perforated tube muffler components, i. theory, *Journal of the Acoustical Society of America* 66 (1979) 772–778.

[2] J. Kergomard, A. Khetabi, X. Mouton, Propagation of acoustic waves in two waveguides couple by perforations: i. theory, *Acta Acoustica* 2 (1994) 1–16.

[3] E. Dokumaci, A discrete approach for analysis of sound transmission in pipes coupled with compact communicating devices, *Journal of Sound and Vibration* 239 (2001) 679–693.

[4] J.W. Sullivan, M.J. Crocker, Analysis of concentric-tube resonators having unpartitioned cavities, *Journal of the Acoustical Society of America* 64 (1978) 207–215.

[5] M.L. Munjal, K.N. Rao, A.D. Sahasrabudhe, Aeroacoustic analysis of perforated muffler components, *Journal of Sound and Vibration* 114 (1987) 173–188.

[6] K.S. Peat, A numerical decoupling analysis of perforated pipe silencer elements, *Journal of Sound and Vibration* 128 (1988) 199–212.

[7] E. Dokumaci, Matrizant approach to acoustic analysis of perforated multiple pipe mufflers carrying mean flow, *Journal of Sound and Vibration* 191 (1996) 505–518.

[8] P.O.A.L. Davies, M.F. Harrison, H.J. Collins Acoustic modeling of multiple path silencers with experimental validation, *Journal of Sound and Vibration* 200 (2000) 195–225.

[9] Y. Aurégan, M. Leroux, Failures in the discrete models for flow duct with perforations: and experimental investigation, *Journal of Sound and Vibration* 265 (2003) 109–121.

[10] Y. Auregan, R. Starobinski, V. Pagneux, Influence of grazing flow and dissipation effects on the acoustic boundary conditions at a lined wall, *Journal of the Acoustical Society of America* 109 (2001) 59–64.

[11] E. Dokumaci, On propagation of plane sound waves in ducts carrying an incompressible axial mean flow having an arbitrary velocity profile, *Journal of Sound Vibration* 249 (2002) 824–827.

[12] E. Dokumaci, Sound transmission in mufflers with multiple perforated co-axial pipes, *Journal of Sound and Vibration* 247 (2001) 379–387.